Active Antenna Array Lumped Ring Configuration

Denver E. J. Humphrey, *Member, IEEE*, and Vincent F. Fusco, *Senior Member, IEEE*

***Abstract*—Coupled active antenna oscillator arrays are used for power-combining at microwave and millimeter-wave frequencies. It is known that relative phase determined by element separation distance ultimately determines the array operational mode and, hence, far-field radiation characteristics. Separately, it is known that coupled oscillator modal stability is achieved by coupling oscillators through lumped capacitive elements. In this paper, an arrangement whereby lumped capacitive elements (placed across the oscillator loads) and radiative coupling are employed concurrently is investigated. The arrangement takes the form of a ring of coupled oscillators used to excite a 2 × 2 antenna array. The effect that these couplings have on array behavior are evaluated using time-domain analysis and analytically derived equations. Experimental results for far-field radiation patterns are discussed in relation to coupled oscillator dynamical behavior. These suggest that the theoretical predictions are valid, offering a robust design tool for studies of larger power-combining arrays.**

***Index Terms*—Antenna arrays.**

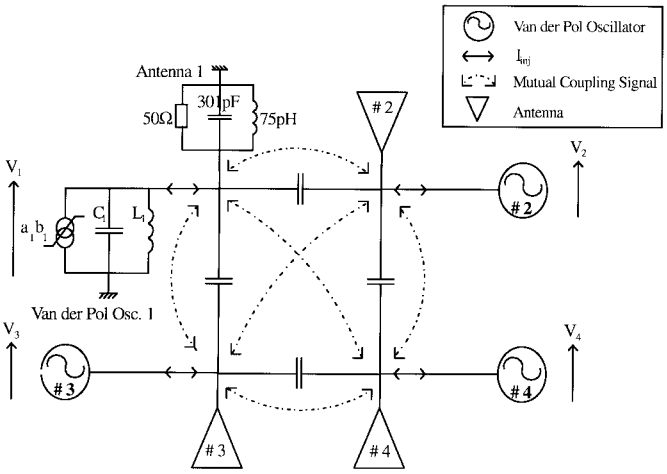

Fig. 1. Ring oscillator electrical arrangement.

I. Introduction

THE growth in the requirement for RF power sources at microwave frequencies for low-cost spacial power combining in personal communications and radar systems has been considerable [1]–[3]. Recent work has involved the use of active antenna power-combining techniques to produce higher output powers [4], [5] from low-power sources.

This paper introduces a system of oscillators placed in a ring configuration whose output ports are coupled with capacitors C and microstrip patch antennas that act as the oscillator loads (Fig. 1). The coupled oscillators behave so as to injection lock each other into a stable in-phase mode, giving spatial combination in the array far field. For the array architecture considered in this paper, two methods of coupling exist concurrently:

1) spatial mutual coupling [5] between antenna elements;
2) lumped element capacitive coupling [6] between oscillator elements.

The advantage here is that the arrangement considerably reduces corporate feed requirements when the 2 × 2 array discussed here is used as a building block in a larger array.

In this paper, an analysis is presented for the ring oscillator system. Here, each oscillator is approximated by an adapted Van der Pol oscillator model [7, Fig. 1]. The predicted dynamical behavior of this model suggests a dominant in-phase mode preference for identical or similar oscillators. This finding establishes the basic utility of the ring-coupled oscillator configuration as a multiport power source in an in-phase power-combining array.

A modified time-domain analysis [8] incorporating the free-space coupling between the antenna elements shows that the inclusion of radiative coupling does not destabilize the dominant mode established by the capacitive coupling network. This is unlike active antenna arrays controlled only by mutual coupling, where mode stability is very dependent on the coupling characteristics [9].

II. Theoretical Considerations

An active antenna element can be modeled by a Van der Pol type model [10], [11]; the model described in this paper is that presented in [10]. In this paper, we have made the antenna element the output load for the Van der Pol oscillator (Fig. 1). Here, the nonlinear current source i representing the active device is

$$i = -aV + b|V|^2V \tag{1}$$

where V is the oscillator output voltage across the load. Coefficients a and b are positive constants, evaluated by fitting the simulated current flowing into the load port of a single isolated oscillator as a function of the magnitude of a virtual voltage source connected at this port with the load removed.

Manuscript received July 29, 1997; revised January 8, 1998. This work was funded by the U.K. Engineering and Physical Science Research Council.

The authors are with the High-Frequency Electronics Laboratory, Department of Electrical and Electronic Engineering, The Queen's University of Belfast, Ashby Buildings, Belfast, BT9 5AH, N. Ireland, U.K.

Publisher Item Identifier S 0018-926X(98)06871-9.

The model shown in Fig. 1 can be analyzed using Kirchoff's laws to form a Van der Pol equation [7]

$$I_{inj} = i + C\frac{dV}{dt} + \frac{1}{L}\int V dt + \frac{V}{R_L} \tag{2}$$

where I_{inj} represents the injected current from both the lumped and mutual coupling networks. Equation (2) is rearranged to form

$$\frac{dV}{dt} + \omega_o^2 \int V dt + \frac{\omega_o V}{Q}[1 + R_L(-a + bA^2)] = \frac{I_{inj}}{C} \tag{3}$$

where

$$V = Ae^{j(\omega_L t + \varphi)} \tag{4}$$

$$\omega_o^2 = \frac{1}{LC} \tag{5}$$

$$Q = \omega_o RC. \tag{6}$$

By inserting (4)–(6) into (3) and following the solution procedure in [12] after equating real and imaginary parts for the kth oscillator, the decoupled amplitude and phase dynamics are formed for the ring-coupled oscillator configuration

$$\frac{dA_k}{dt} + \frac{\omega_k}{2Q_k}A_k[1 + R_{Lk}(-a_k + b_k A_k^2)] = \frac{I_{Rinjk}}{2C_k} \tag{7}$$

$$\frac{d\varphi_k}{dt} + \omega_L - \omega_k = \frac{I_{Iinjk}}{2A_k C_k} \tag{8}$$

where I_{Rinjk} and I_{Iinjk} are the real and imaginary components of the injection current respectively, Q_k is the oscillator Q-factor, C_k is the Van der Pol capacitance, R_{Lk} is the oscillator load, ω_L is the injection-locked frequency and ω_k is the free-running oscillator frequency. External injection-locking can be allowed at the load (R_{Lk}) of each oscillator. Other injection-locking currents are provided by the unsynchronized oscillator induced currents flowing through the lumped coupling impedances and/or by the phase delayed mutual coupling between array elements. Therefore, lumped coupling element is written in terms of real and imaginary components (assumed to have the form of a conductance G_{kl} and a susceptance B_{kl}), while the interelement mutual coupling, as described by York [13, eqs. (13), (14)], is expressed in terms of magnitude and phase. Under these conditions, (7) and (8) are rewritten as

$$\frac{dA_k}{dt} + \frac{\omega_k}{2Q_k}A_k[1 + R_{Lk}(-a_k + b_k A_k^2)] = \frac{1}{2C_k}\Bigg[D_k \cos(\theta_k - \varphi_k) + \sum_{\substack{l=1 \\ l\neq k}}^{N} A_l[G_{kl}\cos(\varphi_l - \varphi_k) - B_{kl}\sin(\varphi_l - \varphi_k) - A_k G_{kl} + \lambda_{lk}\cos(\varphi_l - \varphi_k - \psi_{lk})]\Bigg] \tag{9}$$

$$\frac{d\varphi_k}{dt} + \omega_L - \omega_k = \frac{1}{2A_k C_k}\Bigg[D_k \sin(\theta_k - \varphi_k) + \sum_{\substack{l=1 \\ l\neq k}}^{N} A_l[G_{kl}\sin(\varphi_l - \varphi_k) + B_{kl}\cos(\varphi_l - \varphi_k) - A_k B_{kl} + \lambda_{lk}\sin(\varphi_l - \varphi_k + \psi_{lk})]\Bigg] \tag{10}$$

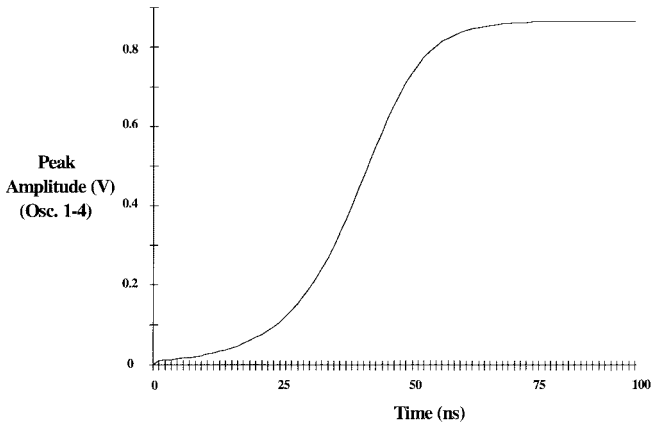

Fig. 2. Dynamical response.

where $D_k e^{j(\omega_L t + \theta_k)}$ represents the injection-locking element from an external source to the kth oscillator. The terms λ_{lk} and ψ_{lk} are the magnitude and phase coefficients of the mutual coupling signal between the lth and kth oscillators, respectively. The inclusion of the terms in D_k enables a single oscillator to be injection locked and its effect on the whole array to be evaluated if required. This is presently the subject of further investigations.

Two numerical methods exist whereby the behavior of the oscillator arrangement can be estimated. The first method is to solve (9) and (10) using Runge–Kutta methods [14]. This yields useful start-up information.

Using this procedure, the simulated start up procedure for a 1-GHz identical oscillator ring is shown in Fig. 2. Here, steady-state operation is achieved for all oscillators after 70 ns. It is important to note that for the identical oscillator scenario, the start up time can be calculated since the steady-state entrained frequency is known and can be accurately evaluated in (10). For nonidentical oscillators, the entrained frequency is both unknown and variable during start up.

The second method used determines the steady-state output behavior of the system. At steady state

$$\frac{dA_k}{dt} = 0 \tag{11}$$

and:

$$\frac{d\varphi_k}{dt} = 0. \tag{12}$$

By substitution of (11) and (12) into (9) and (10) and equating these to zero, the quantities A_k, φ_k, and ω_L can be found by least-squares optimization such that a solution residual value of less that 0.0001 exists.

Thus, the steady-state entrained frequency ω_L, the individual peak amplitudes A_k, and the relative phases (with regard to the first oscillator) φ_k can be calculated.

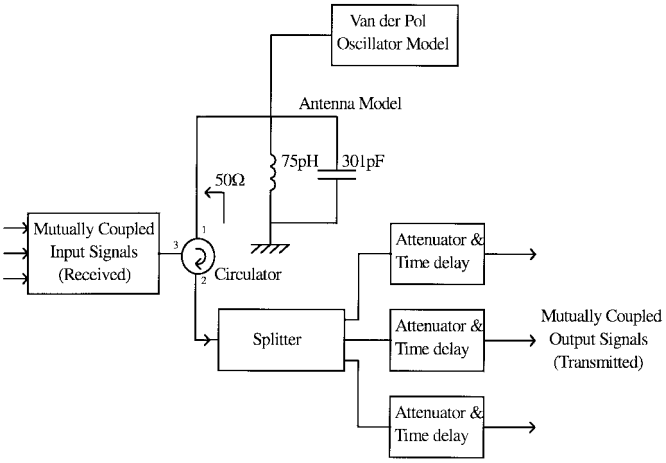

Fig. 3. Mutual coupling array model.

III. Time-Domain Simulation

The Van der Pol circuit model [7] has been implemented in a time-domain simulator [8] in order to determine the model's modal stability behavior over time. Here, a lumped antenna model of the 1-GHz microstrip patch antenna as suggested by Richards [15] and characterized for operation at the Van der Pol circuit resonant frequency is implemented, Fig. 1. In addition, the radiated mutual coupling introduced between the coupled patch antennas introduces a time delayed and attenuated signal [13]; this is applied to each antenna across the array.

The radiative coupling equations are for magnitude

$$\left|\frac{V_2}{V_1}\right|(d_{kl}) = \lambda_{kl} = \frac{C}{k_o d_{kl}} \tag{13}$$

and for phase

$$\psi(d_{kl}) = k_o d_{kl} + \phi \tag{14}$$

where $k_o = \omega_L/c$, c is the speed of light, d_{kl} is the separation distance between elements k and l, C is a fitted constant (typically having a value of 0.12), and ϕ is an added phase term used to account for near-field effects.

For the purpose of the simulation, radiative coupling is implemented by incorporating a circulator as an apparent 50-Ω load for the patch antenna (Fig. 3). This enables the provision for simultaneous transmission and reception of mutual coupling signals to and from the other elements in the array. In this model, mutual coupling between array elements is incorporated in both E and H-planes.

For a 2 $\times$ 2 array each element requires three coupling signals to be added and recovered, one for each of the other antenna elements relative to the element affected by the mutual coupling signal considerations. Hence, the transmitted output signal, i.e., port 2 of the circulator, is split using ideal power splitters (Fig. 3). These signals are then weighted using (13) and (14) and implemented using appropriate circuit-equivalent simulation elements [8]. In addition, on receive, the combined mutually coupled signals from the other antenna elements are summed using a combiner connected to port 3 of the circulator. This, is in turn, connected to the Van der Pol [7] oscillator model. Thus, a system exists whereby both coupling mechanisms can be represented by equivalent circuit models.

TABLE I
Measured Mutual Coupling Between Antenna Elements

s12 = s21	s13 = s31	s14 = s41
0.086 ∠-87.910	0.061 ∠-153.260	0.030 ∠116.930
	s23 = s32	s24 = s42
	0.009 ∠-117.770	0.062 ∠-156.690
		s34 = s43
		0.089 ∠-81.090

For the array considered in this work, the parameters C and ϕ in (13) and (14) are calibrated to the actual array by fitting the actual s-parameter measurements made between antennas at $\lambda/2$ element spacing [16]. For example, in Table I, between elements 1 and 3, $C = 0.191$ (since $d_{13} = \lambda/2$ and $|\lambda_{13}| = 0.061$) and similarly $\phi = 0.466$ rad.

Simulation of the array spaced at a known antiphase separation and no capacitive coupling showed that the starting phases and magnitudes of each oscillator are unsynchronized and, after about 150 ns, they settle to the antiphase mode. However, with the capacitive ring network applied, in-phase operation occurs. Here, the capacitor network provides a pathway for clockwise and anticlockwise ac currents around the ring. Initially, the flow in one direction dominates with the result that over time each oscillator will receive an injection-locking signal from its nearest neighbors. From Kurokawa [17], this modifies oscillator output power and relative phase. Eventually, the opposing currents balance as the oscillators become synchronized and in-phase operation ensues.

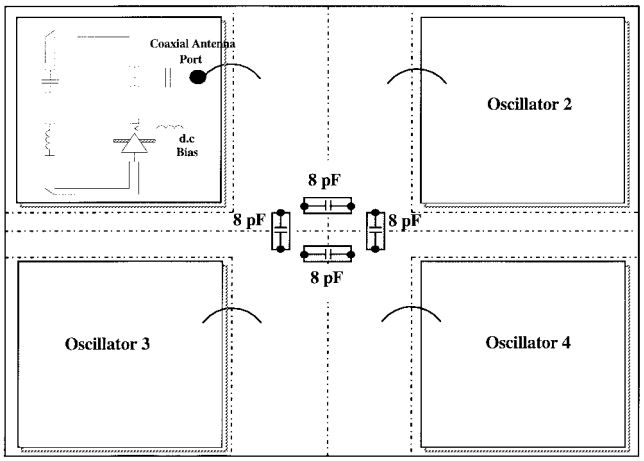

Fig. 4. Oscillator physical arrangement.

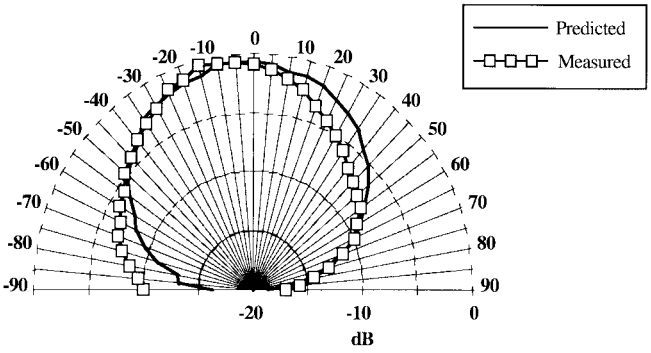

Fig. 5. E-plane measurement and simulation.

IV. Experimental Confirmation

In order to confirm the theoretical predictions, four nonidentical 1-GHz oscillators previously designed in [6] were used to excite the 2×2 array. Separate monolithic integrated circuit (MIC) feedback oscillators [6] built on RT-Duroid [18] were brought together into a larger module (Fig. 4) and coupled using 8-pF chip capacitors connected to separate copper pads in order to equalize reactive phase delays. Each antenna (constructed on 1.6-mm thickness, $\varepsilon_r = 4.55$ material) was matched for 50-Ω operation at 1 GHz; so chosen for ease of experimental confirmation. The normalized E-plane predicted and measured patterns are shown in Fig. 5. The predicted pattern is obtained by measuring the individual power levels of each oscillator first separately, then in pairs, and finally, with all four combined. For each measurement pair, a vector diagram was constructed. From these diagrams, consideration of the parallelogram law yields the amplitude and phase relationships between each of the oscillators in the network. Table II shows this result.

Here, the oscillators are unbalanced due to physical differences in the active devices. This ultimately leads to deviations from the perfect in-phase mode condition predicted for identical oscillators.

The data in Table II is used in a passive array-factor calculation, together with the antenna far-field radiation pattern

TABLE II
Amplitude/Phase Response of Coupled Oscillators

	Measured		Time Domain Simulation		Analytical Calculation	
P1m = 7.71 dBm	Pn/P1m,	deg	Pn/P1m,	deg	Pn/P1m,	deg
Oscillator N = 1	1.00,	0	1.00,	0	0.87,	0
Oscillator N = 2	0.98,	8.1	0.99,	2	0.86	7.6
Oscillator N = 3	1.02,	52	1.02,	53	0.89,	52
Oscillator N = 4	1.19,	9	1.19,	2	1.04,	7.6

measurement for an actual single-patch antenna in order to construct the array radiation pattern, Fig. 5. The resultant pattern match illustrates that in-phase power combining is occurring and that apart from edge-diffraction effects, the maximum deviation between the measured and theoretical patterns is 2 dB.

It should be noted that oscillator 3 was detuned relative to the other oscillators in order to ensure an entrained array frequency. This modifies the array factor from the ideal cophased situation since a phase error is induced. However, the overall effect on the resultant radiation pattern prediction is minimal. Hence, similar but nonidentical oscillators can be employed in this array architecture without compromising in-phase power combining functionality.

In addition, it is observed that without the presence of the capacitive ring coupling network a single entrained frequency could not be obtained for the array presented here. That is, a stabilized spatial power combining system could not be established on the basis of mutual free-space coupling inducing locking at approximately half-wavelength array-element separations.

Amplitude normalized time-domain simulation results for the nonidentical oscillators used in the experiment show good correlation to the experimental results (Table II). The actual Van der Pol model parameters used are shown in Table III for the nonidentical oscillators used in the experiment.

When the distributed mutual-coupling mechanisms are removed from the time-domain simulation and when the mutual-coupling terms are neglected from (9) and (10) for the nonidentical oscillator arrangement, all models produce similar results (Table IV). Here, simulated powers are normalized to oscillator 1 (7.71 dBm) predicted by the time-domain model with the mutual coupling on.

From these results the presence of the lumped capacitive coupling elements appear to ensure that the array always starts up and stays in an approximately in-phase power-combining mode and that the free-space coupling has only

TABLE III
VAN DER POL MODEL PARAMETERS

	Oscillator 1	Oscillator 2	Oscillator 3	Oscillator 4
a	21.8962	21.8962	19.3624	20.9657
b	49.4249	50.7411	41.9262	34.8669
C (nF)	105.00	105.00	51.80	105.00
L (pH)	0.214	0.214	0.436	0.214
R_L (Ω)	50	50	50	50
Frequency (GHz)	1.061	1.061	1.059	1.061

TABLE IV
NORMALIZED TIME-DOMAIN SIMULATED OSCILLATOR OUTPUT RESPONSES

P1t = 7.71 dBm	Oscillator 1 Pn/P1t, deg	Oscillator 2 Pn/P1t, deg	Oscillator 3 Pn/P1t, deg	Oscillator 4 Pn/P1t, deg
Coupling ON Time Domain	1.00, 0	0.99, 2	1.02, 53	1.19, 2
Coupling OFF Time Domain	0.99, 0	0.98, 22	1.02, 64	1.18, 8
Coupling ON Analytical	0.87, 0	0.86, 7.6	0.89, 52	1.04, 7.6
Coupling OFF Analytical	0.86, 0	0.85, 7.6	0.89, 52	1.03, 7.6

a small effect on the overall operation of the lumped-coupled array.

Simulated results for an array of identical oscillators (arbitrarily chosen for as oscillator 1 in Table III) results in a perfect in-phase condition.

V. CONCLUSIONS

It was seen that the problem of guaranteeing in-phase spacial power combining in an active array while simultaneously reducing the corporate feed requirements of a passive array, can be resolved by using a ring-coupled oscillator as a synchronized multiport power source. Here, oscillators are coupled using lumped elements to ensure that the likelihood of in-phase frequency entrainment is greatly enhanced when compared to the situation where only spatial mutual coupling between antenna elements exists. Here, the interinjection locking process will not ensure frequency entrainment on the basis of free-space mutual coupling alone.

A mathematical model has been presented that can be implemented and solved for the array to provide dynamical information by virtue of direct numerical simulation of the system dynamical equations. A circuit model permitting direct time-domain simulation of the array was also given. Both provide good agreement to experimental observations.

Identical oscillator elements always obtain the in-phase solution, while nonidentical oscillators are seen to lock into an approximately in-phase condition, thereby ensuring efficient spacial-power combination.

Further work is being carried out in order to determine the beam steering capability of the coupled-oscillator active-array configuration.

ACKNOWLEDGMENT

The authors would like to thank Mr. A. Black for the construction of the circuits used.

REFERENCES

[1] K. Fujimoto, T. Hori, S. Nishimura, and K. Hirasawa, "Applications in mobile and satellite systems," in *Handbook of Microstrip Antennas*, P. S. Hall and J. R. James, Eds. London, U.K.: Peter Peregrinnus, 1989, ch. 18.

[2] R. Schneiderman, "GPS is growing despite competition," *Microwaves RF*, vol. 7, pp. 41–43, Aug. 1992.

[3] A. G. Derneryd, "Resonant microstrip antenna elements and arrays for aerospace applications," in *Handbook of Microstrip Antennas*, P. S. Hall and J. R. James, Eds. London, U.K.: Peter Peregrinnus, 1989, ch. 18.

[4] J. D. Mink, "Quasioptical power combining of solid-state millimeter-wave sources," *IEEE Trans. Microwave Theory Tech.*, vol. MTT-34, pp. 273–279, Feb. 1986.

[5] K. D. Stephan and S. L. Young, "Mode stability of radiation-coupled international locked oscillators for integrated phased arrays," *IEEE Trans. Microwave Theory Tech.*, vol. 36, no. 5, pp. 921–924, May 1988.

[6] D. E. J. Humphrey and V. F. Fusco, "Capacitively coupled array behavior," *Inst. Elect. Eng. Proc. Circuits, Devices, Syst.*, vol. 143, no. 3, pp. 167–170, Apr. 1996.

[7] B. Van der Pol, "The nonlinear theory of electrical oscillations," *Proc. IRE*, vol. 22, pp. 1051–1085, Sept. 1934.

[8] HP MDS™, Hewlett-Packard, Santa Rosa Syst. Div., Santa Rosa, CA 95403 USA.

[9] R. A. York, "Nonlinear analysis of phase relationships in quasi-optical oscillator arrays," *IEEE Trans. Microwave Theory Tech.*, vol. 41, pp. 1799–1809, Oct. 1993.

[10] D. E. J. Humphrey, V. F. Fusco, and S. Drew, "Active antenna array behavior," *IEEE Trans. Microwave Theory Tech.*, vol. 43, pp. 1819–1825, Aug. 1995.

[11] ——, "Active antenna frequency and voltage characteristics," in *Proc. Microwaves Conf.*, London, U.K., Oct. 1994, pp. 272–275.

[12] K. D. Stephan and W. A. Morgan, "Analysis of interinjection-locked oscillators for integrated phased arrays," *IEEE Trans. Antennas Propagat.*, vol. AP-35, pp. 771–781, July 1987.

[13] R. A. York and R. C. Compton, "Measurement and modeling of radiative coupling in oscillator arrays," *IEEE Trans. Microwave Theory Tech.*, vol. 41, pp. 438–444, Mar. 1993.

[14] R. L. Burden and J. D. Faires, *Numerical Analysis.* Boston, MA: PWS-Kent, 1989.

[15] W. F. Richards, Y. T. Lo, and D. D. Harrison, "An improved theory for microstrip antennas and applications," *IEEE Trans. Antennas Propagat.*, vol. AP-29, pp. 38–46, Jan. 1981.

[16] M. Malkomes, "Mutual coupling between microstrip patch antennas," *Electron. Lett.*, vol. 18, no. 12, pp. 520–522, June 1982.

[17] K. Kurokawa, "Microwave solid state oscillator circuits," in *Microwave Devices*, M. J. Howes and D. V. Morgan, Eds. New York: Wiley, 1976, ch. 5.

[18] RT-Duroid 5880, Rogers Corp., Microwave Materials Div., Chandler, AZ 85226 USA.

Denver E. J. Humphrey (M'96) was born in Ballymena, N. Ireland, on July 15, 1972. He received the B.Eng. and the Ph.D. degrees from The Queen's University of Belfast, N. Ireland, in 1993 and 1996.

He has worked for the High-Frequency Electronics Research Group at Queen's University, with a particular interest in active antenna arrays and coupled oscillators. He currently works for Celeritek, U.K., where he is a Design Engineer.

Vincent F. Fusco (S'82–M'82–SM'96) received the B.Sc. (honors), Ph.D., C.Eng., F.I.E.E., and S.M.I.E.E.E. degrees from the Queens University of Belfast, Belfast, N. Ireland, in 1979 and 1982, respectively.

He has worked as a Research Engineer on short-range radar and radio-telemetry systems and is currently Professor of high frequency electronic engineering in the School of Electrical Engineering and Computer Science, The Queens University of Belfast, where he is also Head of the High-Frequency Research Group. He has acted as consultant to a number of companies. He has also published more than 150 research papers and is author of *Microwave Circuits, Analysis and Computer Aided Design* (Englewood Cliffs, NJ: Prentice-Hall, 1987). His current research interests include active antenna design, nonlinear microwave circuit design, and concurrent techniques for electromagnetic field mapping.

Dr. Fusco is a Chartered Electrical Engineer and a member of the Institution of Electrical Engineers (IEE). He is involved with numerous professional committees including the IEE Professional Group E11, Antennas and Propagation.